Tropical Journal of Natural Product Research

Available online at https://www.tjnpr.org

Original Research Article

Molecular Docking Simulation of Reported Phytochemical Compounds from *Curculigo latifolia* Extract on Target Proteins Related to Skin Antiaging

Syamsu Nur[1,2], Muhammad Hanafi[3,4], Heri Setiawan[5], Nursamsiar Nursamsiar[2], Berna Elya[1]*

[1]Department of Phytochemistry and Pharmacognosy, Faculty of Pharmacy, University of Indonesia, Depok, 16424, Indonesia.
[2]Department of Pharmaceutical Chemistry, Sekolah Tinggi Ilmu Farmasi Makassar, Makassar, 90245, Indonesia.
[3]Research Centre for Pharmaceutical Ingredient and Traditional Medicine, National Research and Innovation Agency (BRIN), Serpong, 15314, Indonesia.
[4]Department of Phytochemistry, Faculty of Pharmacy, Pancasila University, South Jakarta, 12640, Indonesia.
[5]Department of Pharmacology, Faculty of Pharmacy, University of Indonesia, Depok, 16424, Indonesia.

ARTICLE INFO

ABSTRACT

Curculigo latifolia Dryand.Ex W. T. Alton is a plant reported to have antioxidant and anti-aging activities. Studies have shown the interaction of compounds from this plant with target proteins associated with antiaging *in silico*. This study therefore examines the *in silico* antiaging activity of selected compounds from *Curculigo latifolia* using unreported target proteins, including elastase, TNF-alpha, and Tyrosinase. Antiaging activity screening of these compounds was carried out *in silico* using AutoDock 14.0 software. A total of forty-six (46) compounds were successfully docked with each target protein. The results showed that the test compounds from *C. latifolia* have good interactions with the target proteins as indicated by their negative binding free energy values. Only a few of the test compounds had the most negative binding free energy values and interacted with the target proteins in a similar fashion as the native ligands. Compounds 4 (mundulone), 11 (orcinol glucoside), 12 (orcinol glucoside B), 14 (curculigoside B), 15 (curculigoside C), 23 (5,2,6-Trihydroxy-7,8 dimethoxyflavone-2-*O*-*β*-D-glucoside), 29 (aviprin), 30 (guaiacol), 34 (quercetin), 38 (monobenzone) and 42 (stigmastan-3,6-dione) were shown to have an inhibitory effect on one target protein, while, compounds 2 (pomiferin) and 40 (frangulin B) were predicted to interact with multitarget proteins. Compounds 2 and 40 tend to fulfill the Lipinski rule, pharmacokinetics, and toxicity requirements *in silico* and therefore could be developed for their potential use as antiaging molecules.

Introduction

The skin is the outermost organ that covers the entire human body and has the function of protecting the body from various harmful substances. However, the skin can experience a complex biological phenomena involving unavoidable and persistent physiological processes that cause skin aging.[1–3] Skin tissue slowly loses its capacity to replenish or regenerate itself, retain its structure, and carry out its usual functions as it ages. Some people age with age, while others experience faster aging, known as premature aging.[4–7] This is due to a combination of intrinsic aging, which is influenced by genetic factors related to chronological age, and extrinsic aging, which is influenced by environmental factors such as UV exposure, smoking, chemicals, and gravity. One of the most important factors in extrinsic aging is ultraviolet radiation (UV), which occurs in photoaging, where repeated exposure to sunlight can lead to reactive oxygen species (ROS) formation.[8–10]

*Corresponding author. E mail: berna.elya@farmasi.ui.ac.id
Tel: +6281314161497

Reactive oxygen species (ROS) contribute significantly to the dermal extracellular matrix changes brought about by intrinsic aging and photoaging from a molecular perspective.[11] Biochemically, in the body, ROS can be produced from a variety of sources, including the mitochondrial electron transport chain, peroxisomal and endoplasmic reticulum (ER) localized proteins, the Fenton reaction, and enzymes such as cyclooxygenase, lipoxygenase, xanthine oxidase, and nicotinamide adenine dinucleotide phosphate (NADPH) oxidase.[12,13] Under normal conditions without ligand, the receptor tyrosine kinase (RTK) activity on the cell surface is inhibited by the receptor protein tyrosine phosphatase (RPTP), which dephosphorylates RTK. However, the cellular chromophore absorbs energy under UV radiation and becomes excited, generating oxidation products and ROS. ROS inhibit RPTP activity by binding to cysteine at the RPTP catalytic site, increasing levels of phosphorylated RTK and triggering downstream signalling pathways, including activation of mitogen-activated protein kinase (MAPK) and nuclear factor-kB (NF-kB) and transcription factor activator protein-1 (AP-1).[3,14] In photoaged skin, activated NF-kB and AP-1 decrease collagen synthesis and enhance MMP gene transcription. In addition, the photoaging effect activates an increase in neutrophil elastase influx as a result of induction of the occurring angiogenesis so that the elastin network is degraded and triggers the appearance of wrinkles on the skin.[15,16] Another effect caused by photoaging is the activation of tyrosinase, which causes the formation of eumelanin and hyperpigmentation clinically associated with aging.[17–19]

Cosmetics are commonly used to deal with premature aging, but most are made of synthetic materials whose continued use causes adverse effects. Products made from natural ingredients with mild side effects needs to be developed as antiaging agents.[20,21] Various plants are rich in antioxidant compounds that can protect the skin from various

negative effects of the environment and biological processes in the body, and therefore prevent premature skin aging.[22] One of the plants that can be developed as an anti-aging drug candidate is *Curculigo latifolia*. *C. latifolia* extract has been reported to have antidiabetic, antibacterial, and potent antioxidant effects. Studies has also reported *C. latifolia* to be rich in antioxidant compounds, and the ability of the extracts from the plant to protect the skin from UV exposure *in vitro* has been demonstrated.[23] Antioxidant activity and protective effects against UV radiation strongly support the development of *C. latifolia* as an anti-aging agent. Several studies have reported that *C. latifolia* contains phenolic compounds, phenolic glycosides, flavonoids, and steroid/terpenoid groups, namely cycloartan derivatives. These compounds have anti-aging activity on the skin.[23,24]

Chemical compounds derived from natural ingredients offer attractive and effective bioactivities, especially anti-aging activity. The structure-based design of drug molecules using phytochemical compounds provides a rapid predictive profile of the compounds' biological activity and reduces the associated ambiguity. Therefore, this research focuses on developing drug candidates that can be used as anti-aging agents from the previously reported phytochemical constituents of *C. latifolia*. The *in silico* molecular docking model was chosen to investigate the binding affinity of the selected compounds to multiple target proteins involved in the mechanism of premature aging. This work may aid in the discovery of candidate compounds with anti-aging activity for future study.

Materials and Methods

Materials
The materials used were the 3D structures of the ligand binding domain (LBD) of elastase, TNF-alpha, and tyrosinase obtained from the Protein Data Bank online database (www.pdb.org) and compounds from *C. latifolia* (Table 1). Compounds from *C. latifolia* were obtained from previously reported studies.[24–28] The instruments used were Acer Aspire-5 computer hardware with a Ryzen 5 processor technical specifications, 8 GB DDR3 memory (RAM), HD Graphics 1080, 15 HD monitor, 500 GB hard drive, and Windows 11 Ultimate operating system. The software package used was Chemdraw Ultra® 8.0 (www.cambridgesoft.com), Hyperchem® 8, ArgusLab® (www.arguslab.com), Discovery Studio® and the AutoDock Tools® application complete with

AutoDock and Autogrid programs.
Ligands Preparation
The ligands used in this study were 46 compounds from the *C. latifolia* plant. The ligand preparation started by creating a 2D structure with the ChemDraw Ultra 8.0 program in the ChemOffice v.8.0 package, followed by a 3D ligand structure created with Chem3D v.8.0 in the ChemOffice v.8.0 package and presented in a *mol file format. The 3D structure was then optimized for geometry using the HyperChem Release v8.07 program. The geometry optimization was performed by adding H and model builds and semi-empirical calculations with an AM1 force field in the HyperChem v8.07 program package with an RMS slope value of 0.001. The optimized ligand structure was then analyzed for its molecular properties, saved as *.hin file format, and converted into a *.pdb file format using the ArgusLab program package for further use in the AutoDock Tools v.4.2 program package. With the aid of the

AutoDock Tools v.4.2 program package, all Hydrogen bonds were added, Gasteiger charges computed and Non-Polar hydrogens were merged, and the file was saved as *.pdbq format, followed by Torsion input to set several torsion angles with selected atoms, which were then saved as *.pdbqt format.[29,30]

Protein preparation
The 3D structures of the enzymes elastase (1B0F), TNF alpha (3EWJ), and tyrosinase (5M8N) as target proteins was presented in the program package Discover Studio Visualizer v17.2.0 (Table 1). The elastase and TNF-alpha proteins were composed of 2 monomers; chain A and chain B, and then chain A was selected for elastase and chain B for TNF-alpha. The chain was separated from water molecule and its natural ligands and saved as the *.pdb file. Protein tyrosinase is a tetramer consisting of 4 monomers; chains A, B, C, and D. Chain B was selected (all chains have the same sequence, so any chain can be selected). The chain structure was separated with the AutoDock Tools 4.2 program and provided with polar hydrogen atoms. At the same time, the partial charge of each atom was calculated using Kollman's add, which is included in the Autodock Tools 4.2 program package. Then the chain structure was saved as a *.pdbqt file.[29,30]

Docking Method Validation
Validation was performed to demonstrate that the selected docking parameters can dock the androgen receptor ligands. Validation was carried out by recoupling natural ligands into the active site of the receptor or protein. Docking was done with the default software conditions, with no changes to run or grid.

Ligand Docking Simulation
Using the AutoDock 4.2 package, a grid was formed with the appropriate dimensions, which was used during the validation process to cover all amino acid residues involved in ligand binding with the enzymes elastase (1B0F), TNF alpha (3EWJ), and tyrosinase (5M8N). The grid was formed at the site of the bound ligand structure. The information about target proteins and ligands and grid dimensions were saved as *.gpf file format. The electrostatic potential map, AutoGrid 4.2 grid map and calculation results were saved as *.glg file format. Docking Tools and Lamarckian GA were selected and saved as *.dpf file format. Docking simulation results were saved as *.dlg file format.[29,30]

Physicochemical, Pharmacokinetic, and Toxicity Profiles of Active Compounds
Analysis of the physicochemical profile, pharmacokinetics and toxicity of the active compounds was continued *in silico* using the https://preadmet.qsarhub.com/ website.

Data Analysis of Docking Simulation
The parameters evaluated consisted of the orientation of the ligand structure, hydrophobic interactions, the hydrogen bond formed, and the free energy value of the molecular docking process of each ligand. Ligand interactions with proteins were visualized in 3D. Each ligand's binding affinity as well as their physicochemical, pharmacokinetic and toxicity predictions were visualized in tabular form, and the ligands that gave the most negative binding affinity were selected and compared with the native ligand.

Table 1: Compounds of *Curculigo latifolia*

Compound No.	Name	Molecular Formula	References
1	Phloridzin	$C_{21}H_{24}O_{10}$	[27]
2	Pomiferin	$C_{25}H_{24}O_6$	[27]
3	Scandenin	$C_{26}H_{26}O_6$	[27]
4	Mundulone	$C_{26}H_{26}O_6$	[27]
5	Dimethylcaffeic acid	$C_{11}H_{12}O_4$	[27]
6	Protocatechuic acid	$C_7H_6O_4$	[48]

| 7 | Syringic acid | $C_9H_{10}O_5$ | [48] |

Table 1: Cont'd

Compound No.	Name	Molecular Formula	References
8	Cinnamic Acid	$C_9H_8O_2$	[48]
9	Ferulic Acid	$C_{10}H_{10}O_4$	[48]
10	Orcinoside H	$C_{27}H_{36}O_{14}$	[26]
11	Orcinol Glucoside	$C_{13}H_{18}O_7$	[24]
12	Orcinol Glucoside B	$C_{15}H_{21}O_8$	[24]
13	Curculigoside A	$C_{22}H_{26}O_{11}$	[26]
14	Curculigoside B	$C_{21}H_{24}O_{11}$	[24]
15	Curculigoside C	$C_{22}H_{26}O_{12}$	[26]
16	Curculigoside D	$C_{22}H_{26}O_{11}$	[26]
17	Curculigenin A	$C_{30}H_{50}O_4$	[24]
18	Curculigosaponin A	$C_{36}H_{60}O_9$	[24]
19	Curculigosaponin D	$C_{42}H_{70}O_{14}$	[24]
20	Curculigosaponin F	$C_{48}H_{80}O_{19}$	[24]
21	Curculigosaponin I	$C_{48}H_{80}O_{18}$	[24]
22	4-0-caffeoylquinic acid-1	$C_{16}H_{18}O_9$	[24]
23	5,2,6-Trihydroxy-7,8 dimethoxyflavone-2-0-β-D-glucoside	$C_{23}H_{22}O_{13}$	[24]
24	5,7,3,5-Tetrahydroxyflavanone	$C_{21}H_{22}O_{11}$	[24]
25	1,1,6-Trimethyl-1,2-dihydronaphthalene	$C_{13}H_{16}$	[24]
26	Malvalic acid	$C_{18}H_{32}O_2$	[24]
27	Methyl-3-hydroxy-4-methoxybenzoate	$C_9H_{10}O_4$	[24]
28	Sugiol	$C_{20}H_{28}O_2$	[24]
29	Aviprin	$C_{16}H_{16}O_6$	[24]
30	Guaiacol	$C_7H_8O_2$	[24]
31	Smilaxin	$C_{17}H_{16}O_6$	[24]
32	3-Tert-butyl-4-methoxyphenol	$C_{11}H_{16}O_2$	[24]
33	Stearidonic acid	$C_{18}H_{28}O_2$	[24]
34	Quercetin	$C_{15}H_{10}O_7$	[24]
35	Azedarachin C	$C_{32}H_{42}O_{10}$	[24]
36	Trichosanic Acid	$C_{18}H_{30}O_2$	[24]
37	Lucialdehyde B	$C_{30}H_{44}O_3$	[24]
38	Monobenzone	$C_{13}H_{12}O_2$	[27]
39	Hidrokuinon	$C_6H_6O_2$	[28]
40	Frangulin B	$C_{20}H_{18}O_9$	[28]
41	Ubiquinone	$C_{59}H_{90}O_4$	[27]
42	Stigmastan 3,6 dione	$C_{29}H_{48}O_2$	[24]
43	2,3-dihydroxypropyl oleate	$C_{21}H_{40}O_4$	[24]
44	Hordatine A	$C_{28}H_{38}N_8O_4$	[28]
45	Emmotin A	$C_{16}H_{22}O_4$	[27]
46	Rubratoksin B	$C_{26}H_{30}O_{11}$	[27]

Results and Discussion

Docking Method Validation
Validation of the analytical method was carried out by redocking native ligands 1-{3-methyl-2-[4-(morpholine-4-carbonyl)-benzoylamino]-butyryl}-pyrrolidine-2-carboxylic acid (3,3,4,4, 4-Penta fluoro-1-isopropyl-2-oxo-butyl)-amide (1), (1S,3R,6S)-4-oxo-6-{4-[(2-phenylquinolin-4-yl)methoxy]phenyl}-5-azaspiro[2.4]heptane-1-carboxylic acid (2), and mimosine (3) at the active sites of the proteins; elastase, TNF alpha, and tyrosinase, respectively. This process aims to compare the position of the native ligand on the target protein to that of the test ligands. The visualization results showed that each ligand has the same conformation as the native ligands (Figure 2).
In the conformational overlay results for each native ligand before and after validation, the RMSD value of native ligands of 1B0F, 3EWJ, and 5M8N were 1.678, 0.78, and 1.65 Å, respectively. These results showed that the conformation of the test ligands resulting from redocking was closed to that of the native ligands. An RMSD value of less than 2 Å indicates that the conformations of the test ligands are close to the native ligands, and that the positions of the atoms in the ligand from the redocking results were not much different from those in the ligand from the crystallography results.[29–32] The results of the validation of the docking method of each ligand for proteins 1B0F, 3EWJ, and 5M8N obtained RMSD values of less than 2 Å with binding free energies (ΔG) values of -7.69, -15.86, and -6.44 kcal/mol, respectively. Each of these interactions used a grid box size of 34×54×20 Å (1B0F), 24×40×44 Å (3EWJ), and 40×40×40 Å (5M8N) with x, y, and z coordinates of 69,048 Å, 51,487 Å, and 55,179 Å for protein 1B0F, -44.320 Å, 25.911 Å, -19,073 Å for protein 3EWJ and 16.34 Å; -5.955 Å; 25,418 Å for protein 5M8N. The size and coordinates of each grid box were implemented for *C. latifolia* ligands. The validation of the docking method with respect to the coordinates and grid box size was slightly different from that of previous studies, however, the resulting RMSD value met the docking requirements with a value less than 2 Å.[33,34]

Binding Interaction
This study used 46 test ligands docked to each target protein. Each test ligand produced 10 conformations ranked based on the best ΔG value and then compared with the amino acids in the native ligands. In addition, this study evaluated the interaction distance of the hydrogen bond formed, which is measured based on its ionization potential, which shows how much energy is needed to remove electrons from the highest molecular orbital to cause electron donor-acceptor transfer between the native ligand and the test ligand.[30,35,36] Formation of many hydrogen bonds indicate a strong interaction between the target protein and either the native ligand or the test ligand. This indicates that the test ligand has similar activity as the native ligand in inhibiting the target protein, thus supporting the action of the test ligand as antiaging agent.[31,37] The results of the docking simulation analysis of the 46 compounds from *C. latifolia* against the target proteins 1B0F, 3EWJ, and 5M8N are presented in Tables 2, 3, and 4.

Table 2: Molecular docking analysis of *C. latifolia* compounds against elastase target protein (1B0F)

Ligands	Molecular docking simulation				
	ΔG value (kcal/mol)	H-bond Donor	H-bond Acceptor	Bond-Distance (Å)	Amino acid residue
NL 1 (1B0F)	-7.69	6	1	2 - 3.2	Phe41, Cys42, His57, Leu99b, Leu167, Phe192, Gly193, Ser195, Ser214, Phe215, Val216, Arg217
Compound 1	-4.84	4	5	1.8 - 3.2	Arg177, Ser195, Val216, Ser214
Compound 2	-8,35	3	1	2 - 3.1	Ser195, Val216
Compound 3	-6.66	2	1	2 – 2.9	Val216, Gly218
Compound 4	-7.60	3	0	2.9 – 3.1	Gly193, Ser195, Val216
Compound 5	-4.99	10	6	1.9 – 2.96	Gly193, Asp194, Ser195, Val216
Compound 6	-4.78	5	3	2 – 3.2	Gly193, Asp194, Ser195, Val216
Compound 7	-5.05	3	2	2 – 2.94	Gly193, Ser195, Val216
Compound 8	-4.72	1	1	1.9 – 3.15	Val216
Compound 9	-5.11	5	2	1.8 – 2.83	Gly193, Asp194, Ser195, Val216
Compound 10	-5.32	6	2	1.9 – 3.12	Gly193, Asp194, Ser195, Val216
Compound 11	-6.03	5	2	1.88 – 3.13	Gly193, Asp194, Ser195, Val216
Compound 12	-6.01	5	1	1.96 – 3.2	Ser195, Val216
Compound 13	-4.90	3	2	1.8 – 2.9	Gly193, Ser195, Val216
Compound 14	-5.18	3	4	1.9 – 2.9	Gly193, Ser195, Val216, Phe41
Compound 15	-3.64	4	1	2 – 2.89	Gly193, Ser195, Val216
Compound 16	-5.59	4	3	1.99 – 3.01	Gly193, Ser195, Val216, His57, Ser214
Compound 17	-6.84	1	1	1.8 – 2.5	Ser195, Ser214
Compound 18	-6.88	2	1	2.2 – 3.1	Ser195, Arg217, Ser214
Compound 19	-6.41	3	2	2.1 – 3.2	Arg177, Ser195, Arg217, Val216, Ser214
Compound 20	-	-	-	-	-
Compound 21	-5.18	1	1	1.8 – 2.88	Rg177, Ser214
Compound 22	-5.27	3	3	2 – 3.14	Ser195, Val216
Compound 23	-4.27	5	2	1.9 – 3.00	Gly193, Ser195, Val216
Compound 24	-5.74	7	4	1.72 – 3.0	Gly193, Api194, Ser195, Ala227, Val216

Table 2: Cont'd

Ligands	Molecular docking simulation				
	ΔG value (kcal/mol)	H-bond Donor	H-bond Acceptor	Bond-Distance (Å)	Amino acid residue
Compound 25	-5.65	-	-	-	-
Compound 26	-3.43	2	0	2.8 – 3.11	Arg177, Arg177
Compound 27	-4.71	3	0	2.8 – 3.05	Gly193, Ser195, Val216
Compound 28	-6.68	2	2	1.7 – 2.62	Gly193, Ser195
Compound 29	-6.46	4	2	1.9 – 3.12	Gly193, Ser195, Val216
Compound 30	-4.18	3	1	2 – 2.6	Gly193, Ser195
Compound 31	-5.26	5	2	2.1 – 3.16	Gly193, Ser195, Val216, Gly218
Compound 32	-5.76	3	1	1.87 – 2.9	Gly193, Ser195, Val216
Compound 33	-4.08	0	1	2.03	Val216
Compound 34	-6.06	6	2	2 – 3.2	Gly193, Asp194, Ser195, Gly219
Compound 35	-5.30	2	0	2.76 – 2.77	Gly193, Ser195
Compound 36	-4.57	2	1	2.12 – 3.21	Gly218, Gly219, Val216
Compound 37	-6.81	1	0	3.14	Ser195
Compound 38	-6.01	5	1	2 – 3.12	Gly193, Asp194, Ser195, Val216
Compound 39	-4.57	2	1	1.9 – 3.15	Arg177, Arg217, Asn180
Compound 40	-5.66	4	2	2 – 3.11	Arg177, Val216
Compound 41	-	-	-	-	-
Compound 42	-8.27	2	0	2.5 – 3.1	Arg217, Gly218
Compound 43	-2.23	2	0	3.1	Arg177, Arg217
Compound 44	-5.21	1	6	2 – 2.74	Val216, Leu167, Cys182, Asn180, Ser195, Ser214
Compound 45	-5.49	2	1	2 – 3.1	Val216, Ser214
Compound 46	-4.43	1	1	1.9 – 2.99	Val216, Val216

Note: (-) indicates that the compound does not interact with the target protein. In the Amino acid residue column, amino acid in bold indicates that the compound interact with the same amino acid as the native ligand.

Several compounds from *C. latifolia* were identified to have the ability to inhibit target proteins elastase, TNF alpha, and tyrosinase. The existence of negative binding free energy values for *C. latifolia* compounds suggest the prediction that *C. latifolia* compounds are able to inhibit the target proteins. In addition, the number of hydrogen bond donors and acceptors also indicates the compound's ability to bind to the target protein. The number of hydrogen bonds formed determines the strength of the interaction between the ligand and the target protein. Ligands with hydrogen bond interaction with target protein provides higher bond stability than ligands that do not have hydrogen bond.[31,38] The active compounds interacting with each target protein generally have hydrogen bonds, so the bonding interaction between the ligand and the protein was more stable.

The docking simulation results as presented in Table 3 show that compounds from *C. latifolia* inhibited the action of elastase (1B0F) *in silico*. This can be observed from the negative bond free energy value generated from the interaction of the ligands with the target protein. Furthermore, a few of the ligands had binding free energy values that were close to that of the native ligand (ΔG -7.69 kcal/mol) with one of the ligands showing a more negative binding free energy value than that of the native ligand. These compounds include compounds 2 (pomiferin), 4 (mundulone), 29 (aviprin), 11 (orcinol glucoside), and 38 (monobenzone), with binding free energy values of -8.35, -7.60, -6.03, -6.46, and -6.01 kcal/mol, respectively. These five compounds were selected not only based on their binding free energies similar to that of the native ligands but also observed based on hydrogen bond interactions with the same key amino acids as the native ligands, namely; Tyr362, Arg374, and Ser394 (Figure 3). Compounds curculigosaponin F (20), 1,1,6-Trimethyl-1,2-dihydro naphthalene

(25), and ubiquinone (41) showed no interaction with the target protein, which means that these compounds were not active in inhibiting elastase enzyme as observed *in silico*. In the docking analysis, it was found that compound 42 (stigmastan-3,6-dione) had a binding free energy value (-8.27 kcal/mol) that was more negative than that of the native ligand, but the interactions with the key amino acids differ from those observed with the native ligand. Although, the absence of a similar interaction does not mean that the compound is inactive, but it may indicate a new mode of interaction that uses new amino acid residues. Therefore, *in vitro* experiment is needed to determine the activity of this compound. However, in this study, this compound was not selected. The interaction between the active ligands from *C. latifolia* and the target protein 1B0F is presented in Figure 3.

The molecular docking of native ligand with protein 3EWJ had a binding free energy value of -13.05 kcal/mol, which interacted via hydrogen bonding with the amino acid residues Leu348 and Gly349. The bond distance between them ranges from 2.86 to 3.0 Å. It was found that there were two hydrogen bond donors and two hydrogen bond acceptors for the 3EWJ amino acid residue. This information was then compared with the interaction that occured between the ligands from the *C. latifolia* and the 3EWJ target protein.

Table 3 shows the molecular docking results of *C. latifolia* compounds with TNF-alpha protein. These results indicated that compound 42 (stigmastan-3,6-dione) and compound 2 (pomiferin) produce binding free energy values of -11.60 and -11.43 kcal/mol, respectively, which are close to that of the native ligand. These compounds have the same hydrogen bonding interactions with the amino acid residues Leu348 and Gly349 as the native ligand. The number of hydrogen bond donors and hydrogen bond acceptors in each compound was similar to that of

the native ligand. This shows that the mechanism of inhibition that occurs in the compounds and the native ligand for the 3EWJ protein are thought to be similar. Apart from compounds 42 and 2, compounds 40 (frangulin B), 15 (curculigoside C), and 23 (5,2,6-Trihydroxy-7,8 dimethoxyflavone-2-0-*β*-D-glucoside) were also found to interact via hydrogen bonding with the amino acid residues Leu348 and Gly349 with binding free energy values of -9.81, -7.99, and -7.81 kcal/mol, respectively. Even though these compounds have similar interaction as the native ligand, the binding free energy values were greater than that of the native ligand. However, this does not rule out the possibility that these compounds can still be categorized as active *in silico* in inhibiting the activity of the 3EWJ target protein.

The results obtained from the docking simulation analysis between the *C. latifolia* ligands and the target protein tyrosinase (5M8N) is shown in Table 4. Forty-three of *C. latifolia* compounds exhibited inhibitory interactions with the target protein with negative binding free energy values. Two of these compounds, including compound 25 (1,1,6-trimethyl-1,2-dihydro naphthalene) and compound 37 (Lucialdehyde B) gave negative ΔG values, but did not have hydrogen bond (polar) interactions with the target protein. Whereas compounds 20 (curculigosaponin F), 21 (curculigosaponin I), and 41 (ubiquinone) did not give good interactions with the target protein, indicating that they are not active *in silico*. However, these results need to be validated through *in vitro* testing.

Although, these compounds exhibited inhibitory interactions with the target protein, not all of them exhibited interactions similar to that of the native ligand (mimosine). Mimosine is a selective tyrosinase inhibitor that interacts well with the target tyrosinase protein.[39]
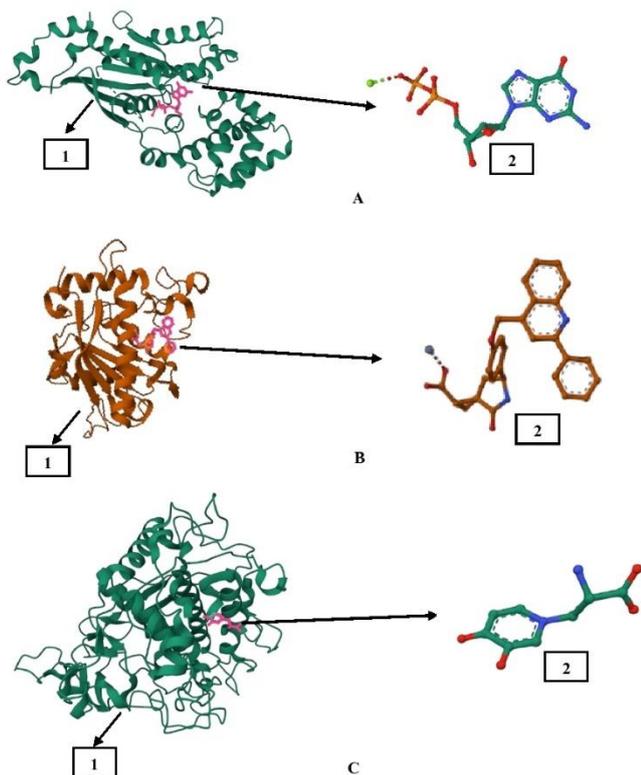
Figure 1: Visualization of elastase (A1) with native ligand 1-{3-methyl-2-[4-(morpholine-4-carbonyl)-benzoylamino]-butyryl}-pyrrolidine-2-carboxylic acid (3,3,4,4,4-pentafluoro-1-isopropyl-2-oxo-butyl)-amide (A2), TNF alpha (B1) with native ligand (1S,3R,6S)-4-oxo-6-{4-[(2-phenylquinolin-4-yl)methoxy]phenyl}-5-azaspiro[2.4]heptane-1-carboxylic acid (B2), and tyrosinase (C1) with native ligand mimosine (C2).
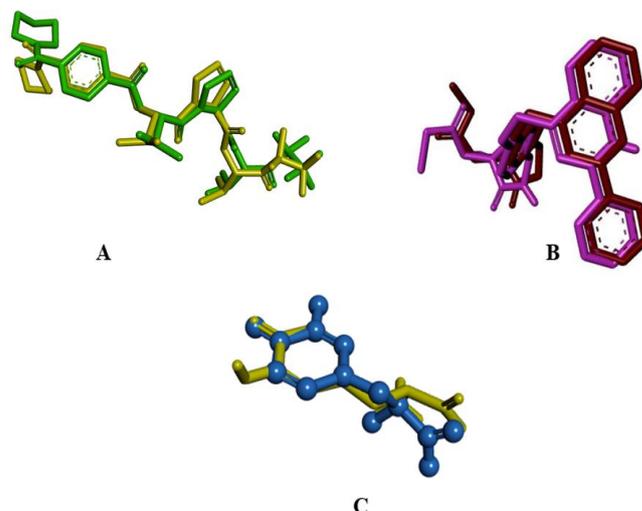
Figure 2: Overlay of test ligand prototype with native ligands. (A): 1-{3-methyl-2-[4-(morpholine-4-carbonyl)-benzoylamino]-butyryl}-pyrrolidine-2-carboxylic acid (3,3,4,4,4-Penta fluoro-1-isopropyl-2-oxo-butyl)-amide (1B0F), (B): (1S,3R,6S)-4-oxo-6-{4-[(2-phenylquinolin-4-yl)methoxy]phenyl}-5-azaspiro[2.4]heptane-1-carboxylic acid (3EWJ), and (C): Mimosine (5M8N).

It is known that the native ligand exhibits interaction with a binding free energy value for the 5M8N protein of -6.44 kcal/mol. Hydrogen bond interactions occur at Tyr362, Arg374, Gln390, Ser394, and Gly388 amino acid residues of 5M8N protein, with the number of hydrogen bond donor and acceptor of 5 and 3, respective, with bond distance between 2.1 -3.2 Å.

From the docking analysis results, compounds 2 (pomiferin), 14 (curculigoside B), 40 (frangulin B), 29 (quercetin), and 12 (orcinol glycoside B) gave binding free energy values close to that of mimosine and some even gave more negative values than mimosine (-6.44 kcal/mol). The five compounds had free energy values of -7.00, -6.52, -6.50, -5.90, and -5.47 kcal/mol, respectively. In addition, the hydrogen bond interactions that occured were generally at the same key amino acids as mimosine, namely Tyr362, Arg374, Gln390, Ser394, and Gly388 (Figure 5). The five compounds also exhibited almost the same number of hydrogen bond donors, acceptors, and bond distance (1.7 – 3.2 Å) as the native ligand.

The docking simulation results show that pomiferin (2) and frangulin B (40) were predicted to act as multitarget ligands. Pomiferin inhibited the activity of the proteins elastase, TNF-alpha, and tyrosinase *in silico* as indicated by their binding free energy values, interactions with residual amino acids, hydrogen bond donors and acceptors which had similarities to each of the native ligands. The compound frangulin B was predicted to inhibit the activity of the target proteins elastase and tyrosinase but not TNF-alpha (Figures 3 and 5). Meanwhile, compounds 4, 11, 12, 14, 15, 23, 29, 34, and 38 were predicted to act on only one of the target proteins (Figures 3, 4, and 5).

The compounds pomiferin and frangulin B act by inhibiting multitarget proteins that are implicated in skin aging. These compounds have been reported to have strong antioxidant effect *in vitro* and *in vivo*. Pomiferin strong antioxidant activity has been ascribed to its phenylated isoflavone moiety.[27] Similarly, frangulin B, a flavonoid derivative rich in hydroxyl groups is a potent free radical scavenger.[40] Their activity as antioxidants *in vitro* and *in vivo* suggests the potential for their use as skin antiaging agents by reducing or inhibiting ROS. In the present study, pomiferin and frangulis B inhibited the induction of enzymatic proteins, including elastase and tyrosinase, as well as TNF-alpha cytokines, which modulate the formation of premature aging. This findings is in line with previous *in silico* studies which showed that pomiferin and frangulin B are inhibitors of multitarget proteins that are implicated in skin aging.[3,27]

Studies have also reported that pomiferin can inhibit the action of collagenase (MMP-13) and gelatinase (MMP-9) *in silico*, both enzymes also have a role in the pathophysiology of skin aging.[3] On the basis of the results obtained from the docking simulation, the two compounds pomiferin and frangulin B have potential to be developed as antiaging agents.

Physicochemical, pharmacokinetics, and toxicity profiles of active compounds

Although, pomiferin and frangulin B are active *in silico* in inhibiting target proteins implicated in skin aging, these compounds need to be further investigated *in vitro* and *in vivo*. In addition, the physicochemical characteristics, pharmacokinetics, and toxicity profiles of these compounds also need to be assessed. Thus, this study conducted an *in silico* assessment of the physicochemical, pharmacokinetics, and toxicity profiles of pomiferin and frangulin B.

Physicochemical evaluation of compounds is done to determine several drug-likeness parameters, including partition coefficient (Log P), molecular weight, hydrogen bond donor, hydrogen bond acceptor, and molar rotation, where these five parameters is known as the Lipinski rule of five. The Lipinski rule provides requirements for drug candidates in the form of molecular weight <500 Da, hydrogen bond donors <5, hydrogen bond acceptors <10, octanol/water partition coefficient (MLogP) <5, rotatable bonds <10, and topological polar surface area (TPSA) <140 Å.[41] The Lipinski rule is a general guide in developing new agents and drug candidates in relation to a molecule's pharmacokinetics parameters and physicochemical properties. The two active compounds (pomiferin and frangulin B) showed remarkable results and complied with Lipinski's rule so that characteristically these two compounds could be developed as new lead molecules with promising biological activity as antiaging agents (Table 5).

Table 3: Molecular docking analysis of *C. latifolia* compounds against TNF-alpha target protein (3EWJ)

Ligands	Molecular docking simulation				
	ΔG value (kcal/mol)	H-bond Donor	H-bond Acceptor	Bond-Distance (Å)	Amino acid residue
NL 2 (3EWJ)	-13.05	2	2	2.86 – 3.0	Leu348, Gly349
Compound 1	-9.43	2	2	2.2 -2.89	Gly394. Asn447
Compound 2	-11.43	2	2	2.89 – 2.91	Leu348, Gly349
Compound 3	-10.46	1	0	1.86	Gly349
Compound 4	-9.71	-	-	-	-
Compound 5	-5.58	3	3	2.2 3.1	His405, Lys432
Compound 6	-4.41	2	3	1.9 – 3.1	His405, Val440
Compound 7	-4.40	0	2	1.8 – 2.3	Ile438, Glu398
Compound 8	-5.13	4	2	0.97 – 3.1	Lys432, lys432, Asn447
Compound 9	-5.70	1	2	1.9 -3.1	Lys432, Val440, Val44
Compound 10	-7.63	3	2	1.87 – 3.2	Se441, Gly442, Glu398
Compound 11	-7.84	2	3	1.88 – 3.3	Ile438,Val440,Tyrr438, Tyr433, Ile438
Compound 12	-8.12	2	2	1.9 – 2.93	His405, Val440,Glu406, Leu401, Asn447
Compound 13	-7.94	3	4	1.8 – 2.91	Ile438,Ala439, Pro437, Met345, Ala439, Gly349
Compound 14	-7.64	3	4	1.8 – 3.1	Leu348, Ile438,, Ala439,Pro437, Tyr436,Glu406
Compound 15	-7.99	5	6	1.7 – 3	Leu348, Gly349, His405, Tyr436, Val440, Glu406, Val434, Tyr433, Ile438
Compound 16	-8.63	1	2	1.9 – 3.2	Val440, Glu406, Glu402
Compound 17	-11.38	1	3	1.8 – 2.7	Gly349, Glu406,Pro437, Met345
Compound 18	-10.97	0	5	1.8 – 2.2	Tyr433, Tyr436, Gly346
Compound 19	-8.37	2	4	1.8 – 2.6	Val440, Ser441, Tyr443, Val440, Tyr246, Gly349
Compound 20	-	-	-	-	-
Compound 21	-0.44	6	3	1.6 2.3	Thr34, Leu348, Asn389, His415, Val440, Gly442, Thr347, Val434, Ile438
Compound 22	-7.18	4	2	1.9 – 3.1	Leu348, Tyr436, Val440, Asn447, Val434, Val440
Compound 23	-7.81	6	3	2.1 – 3.1	Leu348, Gly349, Ala349, Glu406
Compound 24	-8.83	1	4	1.8 – 3.2	Gly349, Ile438, Asn447, Glu406, Pro437
Compound 25	-7.55	-	-	-	-
Compound 26	-5.95	3	1	1.8 – 3.0	Leu348, Gly349

Table 3: Cont'd

Ligands	Molecular docking simulation				
	ΔG value (kcal/mol)	H-bond Donor	H-bond Acceptor	Bond-Distance (Å)	Amino acid residue
Compound 27	-5.95	1	1	2.85	Val440
Compound 28	-10.49	2	1	2.45 – 3.17	Val440, Ser441
Compound 29	-8.51	1	2	1.9 – 2.8	Val440
Compound 30	-4.91	1	1	2.9	Val440
Compound 31	-8.26	0	2	1.93	Glu406, Val440
Compound 32	-6.26	0	1	1.96	Tyr436
Compound 33	-7.16	3	1	2 – 3.1	Leu348, Gly349
Compound 34	-8.72	2	4	1.7 – 3.1	Val402, His405, Asn447, Pro437, Glu406c
Compound 35	-7.65	1	1	2 – 3.1	Thr337, Leu348, Ala439, Gly346
Compound 36	-7.28	3	1	2 – 3.2	Leu348, Gly349
Compound 37	-4.97	-	-	-	-
Compound 38	-7.41	2	1	2.1 – 2.9	Leu348, Gly349
Compound 39	-4.79	1	2	1.8 – 3.1	Val440, Asn447
Compound 40	-9.81	4	2	1.7 – 3.1	Leu348, Gly349, Ile438, Gly349
Compound 41	-	-	-	-	-
Compound 42	-11.60	2	2	2.8 – 3.0	Leu348, Gly349
Compound 43	-7.97	3	2	2 – 3.0	Asn389, Tyr390, Ala439, Met345, Gly346
Compound 44	-9.49	2	8	1.8 – 3.1	Asn389, Val402, Val440, Ile438, Ile438, Val440, Gly346, Ala439, Ala439
Compound 45	-8.51	1	1	2.9	Val440, Val434
Compound 46	-7.98	4	1	2 – 2.9	Asn389, Val402, Val440, Ile438, Ile438, Val440, Gly346, Ala439, Ala439

Note: (-) indicates that the compound does not interact with the target protein. In the Amino acid residue column, amino acid in bold indicates that the compound interact with the same amino acid as the native ligand

In silico pharmacokinetic analysis of pomiferin and frangulin B were evaluated based on the parameters; HIA (Human Intestinal Absorption), Caco2 (Human colon adenocarcinoma), MDCK (Mandin darby canine kidney), plasma protein binding, skin permeability and its interaction with cytochrome P540 (CYP) metabolic enzymes.[42,43] Pomiferin showed positive value in human intestinal absorption (HIA), meaning it can be absorbed in the intestinal tract with bioavailability >30%. *In silico* permeability in Caco 2 cells shows that both compounds have moderate permeability with values ranging from 4 - 70 nm/sec. However, in the MDCK cells the two compounds had weak permeability (<1 x 10^{-6} nm/sec). In terms of distribution, it was observed that pomiferin had a plasma protein binding of >90%, which indicated that the molecule is strongly bound to plasma proteins such that only a small amount is present in the blood, and this suggests that pomiferin might have a toxic effect. The observation was different for frangulin B, which had a plasma protein binding value of 70% (<90%), indicating that amount of this compound that is present in the blood is enough to ellicit an effect. Distribution prediction is normally done using PPB (plasma protein binding) parameters, which is drug fraction available in free form for distribution to different tissues, and by QSAR (Quantitative Structure-Activity Relationship) analysis, which aims to determine the estimated degree of plasma protein binding based on molecular structure parameters and physicochemical properties of compounds.[44,45] In this study, it was found that pomiferin and frangulin B showed low skin permeability. Nevertheless, this does not rule out the possibility of these compounds being developed as drug candidates that can be used orally and topically.

Based on the predictions of their metabolism, pomiferin and frangulin B were found to inhibit CYP2C19, CYP2C9, and CYP3A4. Drugs that are CYP2C19 and CYP2C9 inhibitors can increase plasma concentrations of some drugs and sometimes cause side effects.[46] on the other hand, CYP3A4 are enzymes that play a major role in the metabolism of many small organic molecules (xenobiotics), such as poisons and drugs, and their inhibition increases the plasma concentrations of a number of drugs.[47] Pomiferin and frangulin B are neither inhibitors nor substrates for CYP2D6. Assessment of the CYP parameters indicated that the two active compounds (pomiferin and frangulin B) generally did not adversely affect the metabolic enzymes. Based on the prediction of toxicity through Ames test and mouse model of carcinoma, pomiferin and frangulin B were identified as non-mutagenic.[3]

In contrast, in carcinoma rat model, pomiferin was positively mutagenic. Therefore, this observation should be taken into consideration in the drug development of this compound and if possible, a structure modification of pomiferin should be considered before its development as an antiaging drug candidate.

Conclusion

Curculigo latifolia compounds were successfully docked with elastase, TNF-alpha, and Tyrosinase target proteins. The results of the molecular simulations of forty-six compounds from this plant predicted that several of the compounds have activity in inhibiting the target proteins. However, only compounds 2 (pomiferin) and 40 (frangulin B) were predicted to have the ability to interact with all three target proteins (elastase, TNF-alpha and tyrosinase) with binding free energy and interactions with amino acid residues in a similar fashion as the native ligands. Furthermore, the drug-likeness, pharmacokinetics and toxicity predictions show that pomiferin and frangulin B met the requirements for drug candidates that could be considered for development as antiaging drugs.

Conflict of Interest

The authors declare no conflict of interest.

Authors' Declaration

The authors hereby declare that the work presented in this article is original and that any liability for claims relating to the content of this article will be borne by them.

Native Ligand (1B0F)   Compound 2 (pomiferin)   Compound 4 (mundulone)

Compound 11 (orcinol glycoside)   Compound 29 (aviprin)   Compound 38 (monobenzone)

Interactions

- van der Waals
- Conventional Hydrogen Bond
- Carbon Hydrogen Bond
- Halogen (Fluorine)
- Pi-Pi Stacked
- Alkyl
- Pi-Alkyl
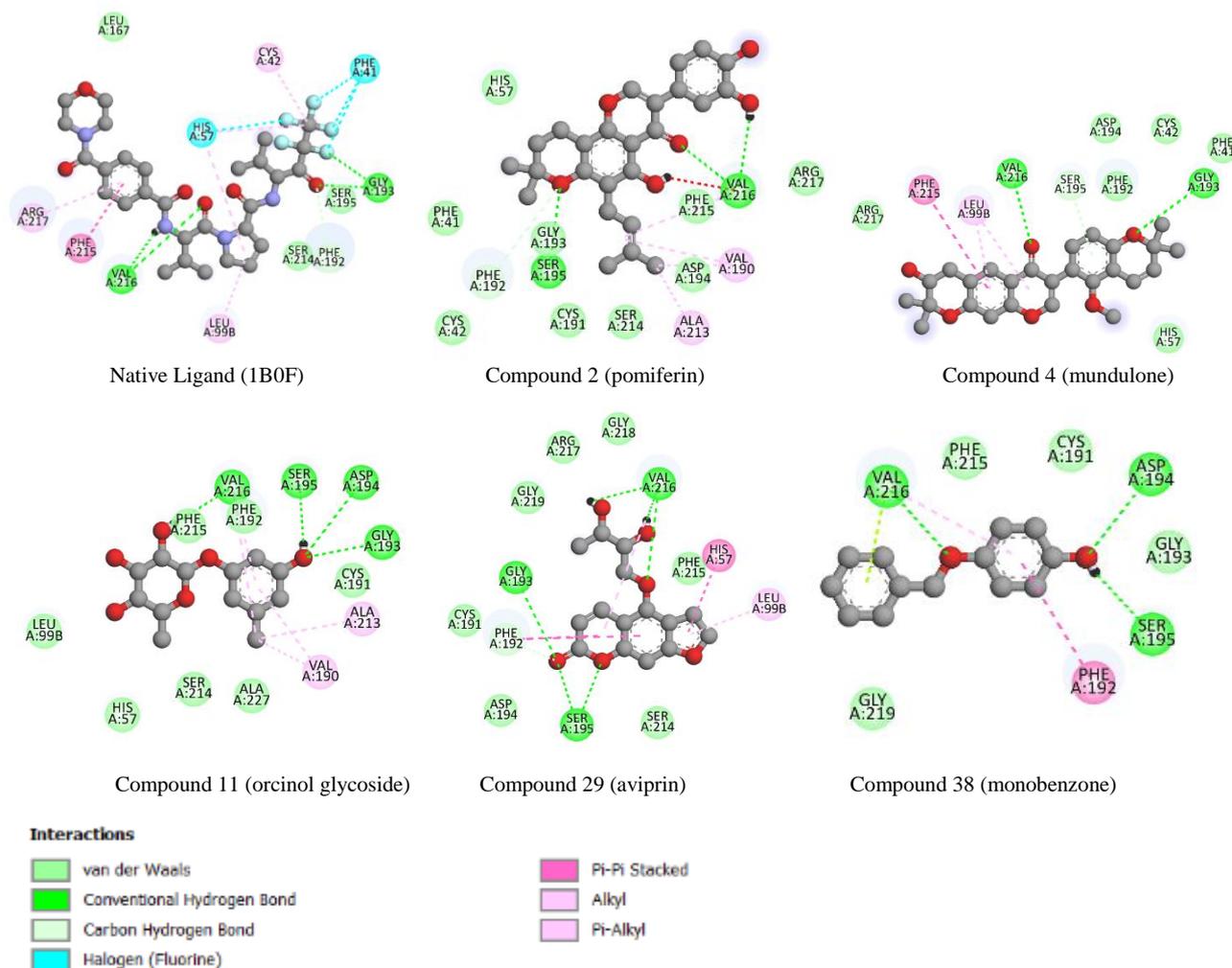
Note: Native ligands interact via hydrogen bond with the amino acids Gly193, Ser195, and Val216; Van der Waals interactions with the amino acids Leu167, Ser214, and Phe192; Pi-pi stacked interactions with Phe215 amino acids; Alkyl/pi-alkyl interactions with Cys42, Leu99b, and Arg217 proteins; Interaction of halogens with the amino acids Phe41 and His57. Generally, compounds 2, 4, 11, 29, and 38 have hydrogen bond and van der Waals interactions similar to the native ligands.

Figure 3: Interaction of native ligand and *C. latifolia* compounds with elastase target protein (1B0F)
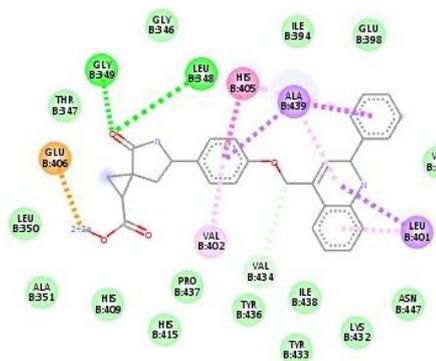
Native Ligan (3EWJ)
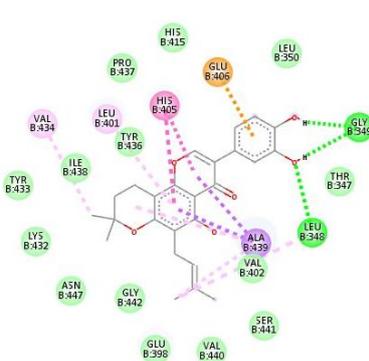
Compound 2 (pomiferin)
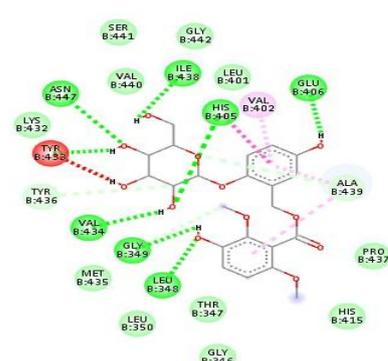
Compound 15 (curculigoside C)
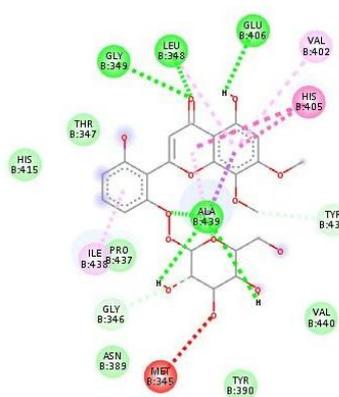
Compound 23
(5,2,6-Trihydroxy-7,8 dimethoxy-
flavone-2-0-β-D-glucoside)
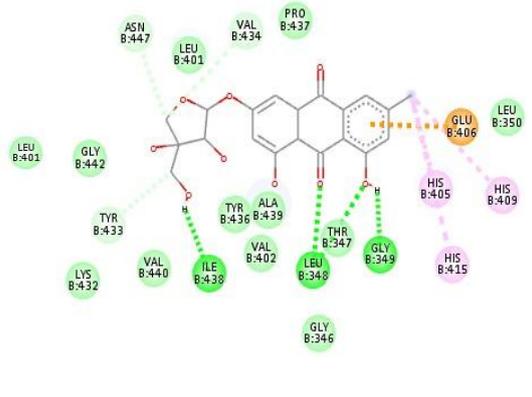
Compound 40 (frangulin B)
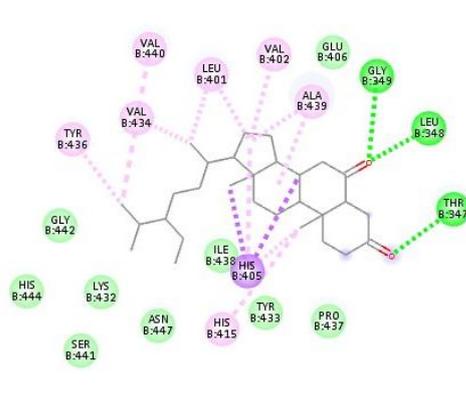
Compound 42 (stigmastan 3,6 dione)

Interactions

van der Waals	Pi-Sigma
Attractive Charge	Pi-Pi Stacked
Conventional Hydrogen Bond	Pi-Alkyl
Carbon Hydrogen Bond	

Note: Native ligands interact via hydrogen bond with amino acid residues Leu348 and Gly349; Van der waals interactions with the amino acids Gly346, Thr347, Leu350, Ala351, Glu398, His415, Tyr433, Val434, Tyr436, Pro437, Ile438, Val440, Ser441, Gly442, and Asn447; pi-sigma Interaction with the amino acids Ala439 and Leu401; pi-alkyl interactions with the amino acid Val402; Pi-pi stacked interactions with His405 amino acids and attractive charge interactions with Glu406. All compounds have similar hydrogen bond and van der Waals interactions with amino acid residues as the native ligands. Meanwhile, the pi-alkyl interactions with the amino acid residue Val402 occurred in compounds 15, 23, and 42 only. Compounds 2 and 40 were found to have the same interaction with the amino acid residue Glu406 (attractive charge) as the native ligand. While, the pi-sigma interaction with His439 occured in compound 2 only and had the same interaction as with the native ligand.

Figure 4: Interaction of native ligand and *C. latifolia* compounds with TNF-alpha target protein (3EWJ)

Table 4: Molecular docking analysis of *C. latifolia* compounds against tyrosinase target protein (5M8N)

Ligands	Molecular docking simulation				
	ΔG value (kcal/mol)	H-bond Donor	H-bond Acceptor	Bond-Distance (Å)	Amino acid residue
NL 3 (5M8N)	-6.44	5	3	2.1 – 3.2	Tyr362, Arg374, Gln390, Ser394, Gly388
Compound 1	-6.34	3	3	2.1 – 3.0	Tyr362, Arg374, Thr391, Asp212, His215
Compound 2	-7.00	5	1	2.2 – 3.1	Tyr362, Arg374, His381, Thr391, Ser394
Compound 3	-8.46	2	2	2.1 2.7	Arg374, Thr391, His192
Compound 4	-5.60	3	0	2.9 – 3.0	Arg321, Thr391
Compound 5	-6.21	5	1	2.2 – 3.1	Tyr362, ISrg374, His381, Ser394
Compound 6	-4.58	5	3	2.1 – 3.0	Tyr362, Arg374, Thr391, Gly389
Compound 7	-4.70	2	1	2.1 – 3.0	Tyr362, Arg374

Table 4: Cont'd

Ligands	Molecular docking simulation				
	ΔG value (kcal/mol)	H-bond Donor	H-bond Acceptor	Bond-Distance (Å)	Amino acid residue
Compound 8	-5.86	3	1	2.1 – 3.1	Tyr362, Arg374
Compound 9	-5.84	5	1	2.1 – 3.1	Tyr362, Arg374, Ser394
Compound 10	-6.21	5	3	1.7 – 3.1	Tyr362, Arg374, Thr391, Gly389
Compound 11	-5.75	4	3	1.9 – 3.1	Tyr362, Arg374, Thr391, Gly389
Compound 12	-5.47	4	2	2 – 3.2	Tyr362, Arg374, His381, Gln390, Gly388
Compound 13	-3.76	4	4	2.1 – 3.0	Arg321, Arg324, Thr391, Gly389, Asn378
Compound 14	-6.52	8	4	2.2 – 3.17	Tyr362, Arg374, His381, Gln390, Gly388, Th391, His392
Compound 15	-4.83	7	4	1.96 – 3.0	Tyr362, Thr391, His392, Asn378, Glu360
Compound 16	-4.93	5	3	2 – 3.0	Tyr362, Arg374, Thr391, Glu216
Compound 17	-6.82	0	2	1.8 – 2.31	Gly389, Asp212
Compound 18	-4.42	4	1	1.9 – 2.9	Tyr362, Arg374, Thr391, His392
Compound 19	-0.29	4	0	2.5 – 2.8	Tyr362, Arg374, Thr391, His392
Compound 20	-	-	-	-	-
Compound 21	-	-	-	-	-
Compound 22	-4.63	7	4	2 – 3.17	Tyr362, Arg374, Thr391, Ser394, Gln390
Compound 23	-5.50	4	4	1.9 – 3.14	Tyr362, Arg374, Thr391, Gly389, Asp212, Val196
Compound 24	-6.74	3	2	1.9 – 3.12	Arg374, His381, Thr391, Gly388, Glu216
Compound 25	-6.71	-	-	-	-
Compound 26	-4.68	3	1	2.3 – 3.12	Tyr362, Arg374
Compound 27	-5.24	3	1	1.97 – 3.2	His381, Gln390, Ser394, Gly388
Compound 28	-7.05	2	1	1.94 – 3.12	Thr391, Asn378
Compound 29	-5.20	3	2	1.82 – 2.96	Arg374, Thr391, Gly389
Compound 30	-4.34	1	1	2.5 – 3	Ser394, Gln390
Compound 31	-6.47	3	1	1.84 – 3.15	Arg374, His381, Thr391, Asn378, Gly389, Glu216
Compound 32	-5.57	1	0	2.5	Thr391
Compound 33	-5.77	4	1	2.2 – 3.2	Tyr362, Arg374
Compound 34	-5.90	6	3	2.2 – 3.1	Tyr362, Arg374, His381, Ser394, Gly388
Compound 35	-5.76	3	1	2 – 3.2	Arg374, Glu216
Compound 36	-5.10	3	1	2 – 3.0	Tyr362, Arg374
Compound 37	-8.52	-	-	-	-
Compound 38	-6.21	2	1	2.1 – 3.14	Tyr362, Arg374
Compound 39	-4.49	1	1	1.8 – 2.67	Thr391
Compound 40	-6.50	7	4	1.67 – 3.1	Tyr362, Arg374, Thr391, His392, Asn378, Gly389
Compound 41	-	-	-	-	-
Compound 42	-8.09	4	0	2.8 – 3.0	His381, Leu382. Thr391
Compound 43	-3.13	2	0	3.01	Arg374
Compound 44	-4.87	4	2	1.82 – 3.2	Arg321, Thr391, His392, Asn378
Compound 45	-6.16	5	2	2.3 -3.2	Arg321, Thr391, His392, Asn378
Compound 46	-7.66	0	2	1-8 -1.97	Arg321, Thr391, His392, Asn378

Note: (-) indicates that the compound does not interact with the target protein. In the Amino acid residue column, amino acid in bold indicates that the compound interact with the same amino acid as the native ligand.
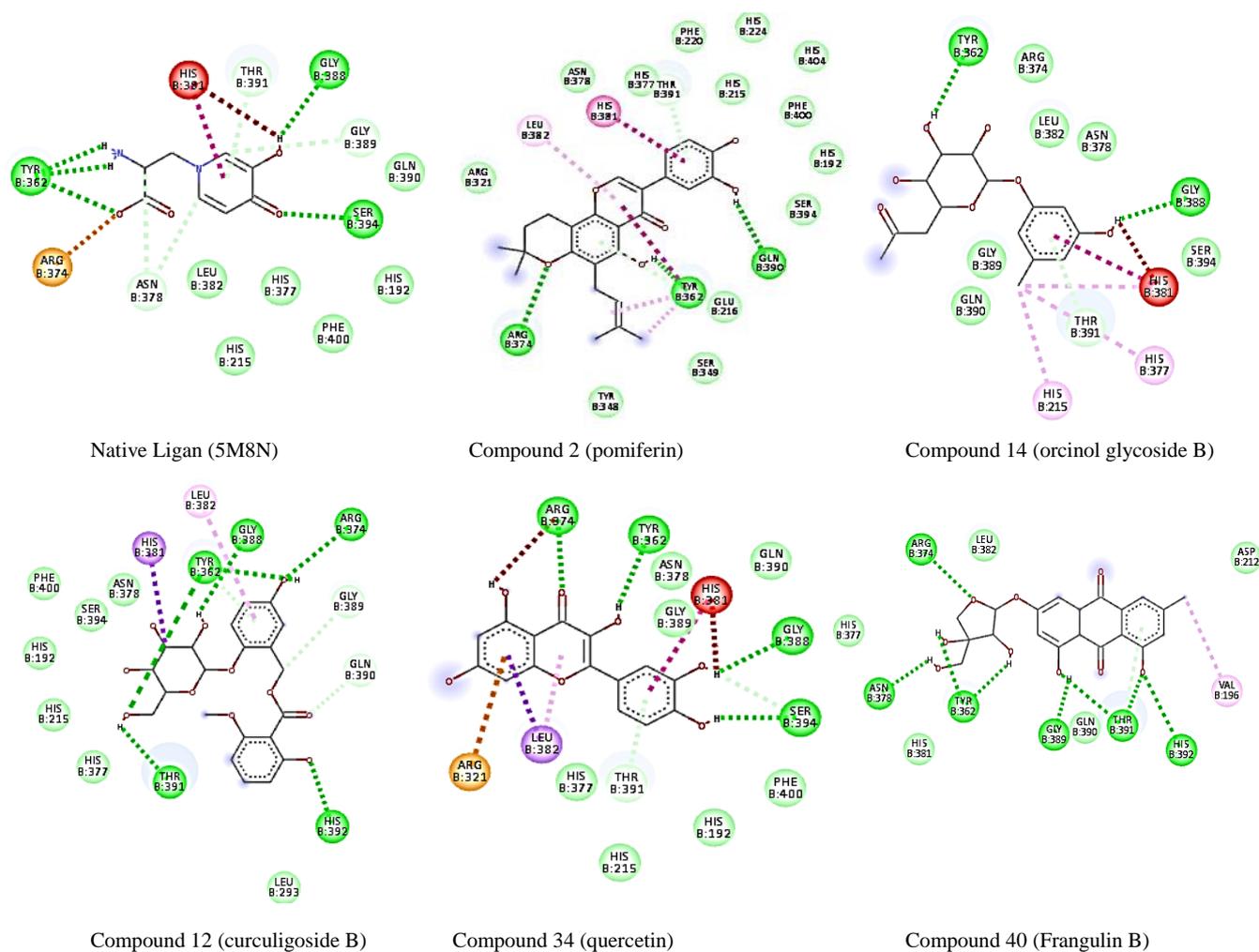
Figure 5: Interaction of native ligand and *C. latifolia* compounds with tyrosinase target protein (5M8N)

Table 5: Druglikeness, Pharmacokinetic and toxicity profile of active compounds from *C. latifolia*

Parameters	Compounds	
	Pomiferin	Frangulin B
Druglikeness (Lipinski rule of five)	Suitable	Suitable
ADME:		
a. HIA	92.5	57.25
b. Caco2	14.7	18.15
c. MDCK	0.051	0.644
d. Plasma protein binding	95.2	71.22
e. Skin permeability	-2.28	-4.47
f. CYP 2C19 inhibition	Inhibitor	Inhibitor
g. CYP 2C9 inhibition	Inhibitor	Inhibitor
h. CYP 2D6 inhibition	No	No

Table 5. Cont'd

Parameters	Compounds	
	Pomiferin	Frangulin B
Druglikeness	Suitable	Suitable
(Lipinski rule of five)		
i. CYP 2D6 Substrat	No	No
j. CYP 3A4 inhibition	Inhibitor	Inhibitor
k. CYP 3A4 substrate	Substrate	Weakly
Toxicity:		
a. Ames Test	Non-mutagenic	Non-mutagenic
b. Carcinoma-Mouse	negative	negative
c. Carcinoma-Rat	Positive	negative

References

1. Zhang S and Duan E. Fighting against Skin Aging: The Way from Bench to Bedside. Cell Transplant. 2018; 27(5):729-738.
2. Yousef H, Alhajj M, Sharma S. Anatomy, Skin (Integument), Epidermis. Stat Pearls Publishing. 2020.
3. Nur S, Angelina AA, Aswad M, Yulianti R, Burhan A, Nursamsiar N. *In vitro* anti-aging activity of *Muntingia calabura* L. fruit extract and its fractions. J Pharm Pharmacogn Res. 2021; 9(4):409–421.
4. Kristianti MT, Goenawan H, Achadiyani A, Sylviana N, Lesmana R. The Potential Role of Vitamin D Administration in The Skin Aging Process Through The Inflammatory Pathway: A Systematic Review. Trop J Nat Prod Res. 2023; 7(4):2675–2681.
5. Soeratri W, Indrajaya S, Hariyadi DM. Ubiquinone-Nanostructured Lipid Carriers Hydrogel Mask for Antiaging: the Journey so Far. Trop J Nat Prod Res. 2020; 4(11):866–876.
6. Anggraini NB, Elya B, Iskandarsyah I. Antielastase Activity of Macassar Kernels (*Rhus javanica*) Stem Extract and Skin Elasticity Evaluation of Its Topical Gel Formulation. Adv Pharmacol Pharm Sci. 2021; 2021:6690029.
7. Lukitaningsih E, Nur S, Qonithah F, Zulbayu A, Kuswahyuning R, Rumiyati R. *In vitro* anti-wrinkle and tyrosinase inhibitory activities of grapefruit peel and strawberry extracts. Trad Med J. 2020; 25(3):182–189.
8. Nur S, Aswad M, Yulianty R, Burhan A, Khairi N, Sami FJ, Nursamsiar. The antioxidant and anti-ageing activity of lyophilisate kersen (*Muntingia calabura* L) fruit *in vitro*. Food Res. 2023; 7(2):23-30.
9. Azwanida ZN, Jonathan OE, Melanie-Jaynes H. Antioxidant, Anti-Collagenase, Anti-Elastase and Anti-Tyrosinase Activities of an Aqueous *Cosmos caudatus* Kunth (Asteraceae) Leaf Extract. Trop J Nat Prod Res. 2020; 4(12):1124–1130.
10. Purohit T, He T, Qin Z, Li T, Fisher GJ, Yan Y, Voorhees JJ, Quan T. Smad3-dependent regulation of type I collagen in human dermal fibroblasts: Impact on human skin connective tissue aging. J Dermatol Sci. 2016; 83(1):80-83.
11. Shin JW, Kwon SH, Choi JY, Na JI, Huh CH, Choi HR, Park KC. Molecular Mechanisms of Dermal Aging and Antiaging Approaches. Int J Mol Sci. 2019; 20(9):2126.
12. Snezhkina AV, Kudryavtseva AV, Kardymon OL, Savvateeva MV, Melnikova NV, Krasnov GS, Dmitriev AA. ROS Generation and Antioxidant Defense Systems in Normal and Malignant Cells. Oxid Med Cell Longev. 2019; 2019:6175804.
13. Oh YS, Shin SY, Kim S, Lee KH, Shin JC, Park KM. Comparison of antiaging, anti-melanogenesis effects, and active components of Raspberry (*Rubus occidentalis* L.) extracts according to maturity. J Food Biochem. 2020; 4(11):e13464.
14. Rittié L and Fisher GJ. Natural and sun-induced aging of human skin. Cold Spring Harb Perspect Med. 2015; 5(1):a015370.
15. Kim M and Park HJ. Molecular Mechanisms of Skin Aging and Rejuvenation. In Molecular Mechanisms of the Aging Process and Rejuvenation. Intechopen. 2016.
16. Kim YH, Chung CB, Kim JG, Ko KI, Park SH, Kim JH, Eom SY, Kim YS, Hwang YI, Kim KH. Anti-wrinkle activity of ziyuglycoside I isolated from a *Sanguisorba officinalis* root extract and its application as a cosmeceutical ingredient. Biosci Biotechnol Biochem. 2008; 72(2):303-311.
17. Apak R, Capanoglu E, Shahidi F. Electron transfer-based antioxidant capacity assays and the cupric ion reducing antioxidant capacity (CUPRAC) assay. In: Measurement of Antioxidant Activity & Capacity (eds R. Apak, E. Capanoglu and F. Shahidi). 2017; 57-75p.
18. Apak R, Güçlü K, Ozyürek M, Bektaşoğlu B, Bener M. Cupric ion reducing antioxidant capacity assay for antioxidants in human serum and for hydroxyl radical scavengers. Methods Mol Biol. 2010; 594:215-239.
19. Solano F. Photoprotection and Skin Pigmentation: Melanin-Related Molecules and Some Other New Agents Obtained from Natural Sources. Molecules. 2020; 25(7):1537.
20. Michalak M. Plant-Derived Antioxidants: Significance in Skin Health and the Ageing Process. Int J Mol Sci. 2022; 23(2):585.
21. Hoang HT, Moon J-Y, Lee Y-C. Natural Antioxidants from Plant Extracts in Skincare Cosmetics: Recent Applications, Challenges and Perspectives. Cosmetics. 2021; 8(4):106.
22. Petruk G, Del Giudice R, Rigano MM, Monti DM. Antioxidants from Plants Protect against Skin Photoaging. Oxid Med Cell Longev. 2018; 2018:1454936.
23. Nur S, Setiawan H, Hanafi M, Elya B. *In vitro* ultra violet (UV) protection of *Curculigo latifolia* extract as a sunscreen candidate. IOP Conf. Series: Earth and Environmental Science. 2022.
24. Nur S, Hanafi M, Setiawan H, Nursamsiar, Elya B. *In silico* evaluation of the dermal antiaging activity of *Molineria latifolia* (Dryand. ex W.T. Aiton) Herb. Ex Kurz compounds. J Pharm Pharmacogn Res. 2023; 11(2):325–345.
25. Mad Nasir N, Ezam Shah NS, Zainal NZ, Kassim NK, Faudzi SMM, Hasan H. Combination of Molecular Networking and LC-MS/MS Profiling in Investigating the Interrelationships between the Antioxidant and Antimicrobial Properties of *Curculigo latifolia*. Plants (Basel). 2021; 10(8):1488.
26. Wang Y, Li J, Li N. Phytochemistry and Pharmacological Activity of Plants of Genus Curculigo: An Updated Review Since 2013. Molecules. 2021; 26(11):3396.

27. Zabidi NA, Ishak NA, Hamid M, Ashari SE. Subcritical Water Extraction of Antioxidants from *Curculigo latifolia* Root. J Chem. 2019; 2019:8047191.

28. Zabidi NA, Ishak NA, Hamid M, Ashari SE, Latif MAM. Inhibitory evaluation of *Curculigo latifolia* on α-glucosidase, DPP (IV) and in vitro studies in antidiabetic with molecular docking relevance to type 2 diabetes mellitus. J Enzyme Inhib Med Chem. 2021; 36(1):109-121.

29. Asnawi A, Nedja M, Febrina E, Purwaniati P. Prediction of a Stable Complex of Compounds in the Ethanol Extract of Celery Leaves (*Apium graveolens* L.) Function as a VKORC1 Antagonist. Trop J Nat Prod Res. 2023; *7*(2):2362–2370.

30. Nursamsiar, Siregar M, Awaluddin A, Nurnahari N, Nur S, Febrina E, Asnawi A. Molecular docking and molecular dynamic simulation of the aglycone of curculigoside a and its derivatives as alpha glucosidase inhibitors. Rasayan J Chem. 2020; 13(1):690-698.

31. Nursamsiar, Nur S, Febrina E, Asnawi A, Syafiie S. Synthesis and Inhibitory Activity of Curculigoside A Derivatives as Potential Anti-Diabetic Agents with β-Cell Apoptosis. J Mol Struct. 2022; 1265:133292.

32. Kontoyianni M, McClellan LM, Sokol GS. Evaluation of docking performance: comparative data on docking algorithms. J Med Chem. 2004; 47(3):558-565.

33. Muflihunna A and Sukmawati S. *In silico* study of java wood (*Lannea coromadelica*) as anti- inflammatory in tnf-α and cox-2 mediators. Indon J Pharm Sci Technol. 2023; 1(1):42-50.

34. Suharti N, Sari MR, Dillasamola D, Putra PP. *In Silico* and *In Vitro* Study of The Ethanol Extract of The White Garland Lily (*Hedychium coronarium* J. Koenig) as a Tyrosinase Inhibitor. Trop J Nat Prod Res. 2023; 7(6):3125–3129.

35. Adetobi ET, Akinsuyi SO, Ahmed OA, Folajimi EO, Babalola BA. *In silico* Evaluation of the Inhibitory Potential of Cymbopogonol from *Cymbopogon citratus* Towards Falcipain-2 (FP2) Cysteine Protease of *Plasmodium falciparum*. Trop J Nat Prod Res. 2022; *6*(10):1687–1684.

36. Pratami MP, Fendiyanto MH, Satrio RD, Nikmah IA, Awwanah M, Farah N, Sari NIP, Nurhadiyanta. *In-silico* Genome Editing Identification and Functional Protein Change of *Chlamydomonas reinhardtii* Acetyl-CoA Carboxylase (CrACCase). Jordan J Biol Sci. 2022; 15(3):431-440.

37. Savitri AD, Hidayati HB, Veterini L, Widyaswari MS, Muhammad AR, Fairus A, Zulfikar MQB, Astri M, Ramasima NA, Anggraeni DP, Nainatika RSA, Juliana. An In-Silico Study on Allicin Compound in Garlic (*Allium Sativum*) as A Potential Inhibitor of Human Epidermal Growth Factor Receptor (Her)-2 Positive Breast Cancer. Jordan J Biol Sci. 2023; 16(1):7-12.

38. Chen D, Oezguen N, Urvil P, Ferguson C, Dann SM, Savidge TC. Regulation of protein-ligand binding affinity by hydrogen bond pairing. Sci Adv. 2016; 2(3):e1501240.

39. Muslimin L, Zainal TH, Hardianti B, Megawati M, Marwati M. Effect of Solvent Extraction on Antityrosinase and Sun Protection Factor of Mulberry (*Morus alba* L.) Cultivated in Wajo, Indonesia. Trop J Nat Prod Res. 2023; *7*(6):3114–3118.

40. Tims M. Review of Isolation, Identification and Characterization of Allelochemicals/Natural Products. J Nat Prod. 2017.

41. Lipinski CA, Lombardo F, Dominy BW, Feeney PJ. Experimental and computational approaches to estimate solubility and permeability in drug discovery and development settings. Adv Drug Deliv Rev. 2001; 46(1-3):3-26.

42. Adianingsih OR, Khasanah U, Anandhy KD, Yurina V. *In silico* ADME-T and molecular docking study of phytoconstituents from *Tithonia diversifolia* (Hemsl.) A. Gray on various targets of diabetic nephropathy. J Pharm Pharmacogn Res. 2022; 10(4):571–594.

43. Riwu AG, Nugraha J, Purwanto DA, Triyono EA. *In silico* analysis of anti-dengue activity of faloak (*Sterculia quadrifida* R. Br) stem bark compounds. J Pharm Pharmacogn Res. 2022; 10(6):1006–1014.

44. Sun L, Yang H, Li J, Wang T, Li W, Liu G, Tang Y. *In Silico* Prediction of Compounds Binding to Human Plasma Proteins by QSAR Models. Chem Med Chem. 2018; 13(6):572-581.

45. Yuan Y, Chang S, Zhang Z, Li Z, Li S, Xie P, Yau WP, Lin H, Cai W, Zhang Y, Xiang X. A novel strategy for prediction of human plasma protein binding using machine learning techniques. Chemomet Intell Lab Syst. 2020; 199:103962.

46. Lynch T and Price A. The effect of cytochrome P450 metabolism on drug response, interactions, and adverse effects. Am Fam Physician. 2007; 76(3):391-396.

47. Youdim KA, Zayed A, Dickins M, Phipps A, Griffiths M, Darekar A, Hyland R, Fahmi O, Hurst S, Plowchalk DR, Cook J, Guo F, Obach RS. Application of CYP3A4 *in vitro* data to predict clinical drug-drug interactions; predictions of compounds as objects of interaction. Br J Clin Pharmacol. 2008; 65(5):680-692.

48. Ooi DJ, Chan KW, Sarega N, Alitheen NB, Ithnin H, Ismail M. Bioprospecting the Curculigoside-Cinnamic Acid-Rich Fraction from *Molineria latifolia* Rhizome as a Potential Antioxidant Therapeutic Agent. Molecules. 2016; 21(6):682.